Stress relaxation in unentangled and entangled polymer liquids

Avik P. Chatterjee,[a] Phillip L. Geissler, and Roger F. Loring
Department of Chemistry, Baker Laboratory, Cornell University, Ithaca, New York 14853

(Received 19 October 1995; accepted 29 December 1995)

We develop a stochastic model for the dynamics of a dense fluid of flexible linear macromolecules. A polymer is represented by a harmonic chain of beads whose mobilities fluctuate in time between two values. A bead in the low-mobility state does not execute local motions, but may move by a cooperative slithering process involving the entire chain. A bead in the high-mobility state may execute both local and slithering motions. The rate at which the mobilities fluctuate is determined self-consistently as a function of chain length through an ansatz that associates these fluctuations with the configurational relaxation of neighboring molecules. We calculate the viscoelastic shear modulus and the coefficients of shear viscosity and self-diffusion for this model. The coefficient of shear viscosity η shows three regimes of dependence on chain length N. For a fluid of short chains, $\eta \sim N$, in agreement with the Rouse model and with the behavior of laboratory polymers. For a liquid of longer chains, η displays an N dependence that is intermediate between N^3 and N^4, in agreement with laboratory measurements. In the asymptotic limit of large N, $\eta \sim N^3$, in agreement with the prediction of the tube model. © *1996 American Institute of Physics.* [S0021-9606(96)50613-X]

I. INTRODUCTION

The character of viscoelastic relaxation in a dense fluid of linear macromolecules depends strongly on chain length.[1–7] For molecules shorter than a critical length, the coefficient of shear viscosity η is found to be proportional to molecular weight M, in agreement with the prediction of the Rouse model.[3] Fluids composed of molecules longer than this critical length[6,7] have viscosities that scale approximately as $M^{3.4}$. In the tube model,[3,8] the predominant mechanism for center-of-mass translation and configurational relaxation is represented by the motion of a chain confined to a tube. The predictions of this model for a variety of observables show semiquantitative agreement with laboratory and computer experiments.[1,3] The tube model in its original form predicts $\eta \sim M^3$ in the long-chain limit.[3] The discrepancy between this prediction and the results of laboratory measurements has motivated numerous treatments of stress relaxation in fluids of long chain molecules, which may be divided into approaches that retain the basic assumptions of the tube model[2,4,9–13] and those that replace the tube model with a different paradigm.[14–19]

The analysis of the tube model that leads to the M^3 scaling of η is based on a consideration of the motion of the chain's center of mass, neglecting the relaxation of intramolecular modes.[3] Both theoretical analysis[9,21] and simulation[11,12,20] have demonstrated that the inclusion of the effects of such modes leads to a prediction for η that displays an M dependence stronger than M^3 but weaker than M^4 for intermediate values of M and which crosses over to an asymptotic M^3 behavior. This finding agrees with the conjecture of Graessley,[22] who noted that the tube model overestimates η relative to laboratory measurements and proposed that the laboratory polymers studied were not sufficiently long to display asymptotic behavior. A different approach to interpreting the exponent 3.4 was taken by Weiss *et al.*, whose calculation of stress relaxation as a multichain rather than a single-chain phenomenon yielded a viscosity exponent of 10/3.[23] A similar consideration underlies the ''double-reptation'' theory of the viscoelastic shear modulus developed by des Cloizeaux.[10] Since the original version of the tube model treats the environment of a molecule as strictly static, several approaches have been developed to incorporate dynamics of the environment into the tube model.[2,22] These treatments include the model of Rubinstein and Colby,[4] in which the tube is treated as a Rouse chain whose beads have randomly assigned static mobilities, and that of Watanabe and Tirrell,[13] in which the rate of tube relaxation varies along the tube.

Several recent descriptions of relaxation in dense polymer fluids present alternatives to the tube picture.[14–19] Schweizer[17] has developed a treatment of dynamics in dense polymer liquids that generalizes molecular theories of the structure and dynamics of simple fluids. This mode-coupling strategy yields a generalized Langevin equation with a spatially nonlocal memory kernel that is evaluated from a molecular derivation. Herman has developed a stochastic model whose assumptions challenge those of the tube picture.[16] In this description, chains move predominantly through the diffusion of mutual points of contact laterally along the chain backbones.

We have developed two related models of polymer dynamics that do not employ the tube hypothesis. In the freely jointed chain (FJC) model, a chain composed of rigid bonds moves by two competing dynamical processes.[24] The first of these is a local conformational change that proceeds by a kink–jump motion whose rate is a stochastic variable that fluctuates between zero and a finite value. These fluctuations mimic dynamics in the environment of the chain. The second

[a]Present address: Department of Materials Science and Engineering, University of Illinois, Urbana, IL 61801.

 0021-9606/96/104(13)/5284/10/$10.00

dynamical process is a slithering motion whose rate is inversely proportional to the chain length. This mode of motion is unaffected by the fluctuations that control the local conformational changes. The rate at which the medium variables fluctuate is determined self-consistently by equating it to the rate of the slowest conformational relaxation process of a chain. We have related the calculation of several observables for this model to solutions of random walks with dynamical disorder on a variety of lattices.[25–27] These are stochastic processes in which the hopping rate of the walker fluctuates in time. We have adapted the effective medium approximation (EMA) of Harrison and Zwanzig[25] and of Sahimi[26] to treat the random walks that are relevant to calculations with the FJC model. Our calculations of the molecular weight dependence of the self-diffusion coefficient[24(e)] and of the time and wave vector dependence of the dynamic structure factor[24(f)] have been shown to agree well with results of laboratory experiment and computer simulation. Calculation of viscoelastic properties for the FJC model is complicated by the forces of constraint associated with the rigid bonds. In Ref. 24(b), Szleifer and Loring related the calculation of the shear modulus $G(t)$ to a two-dimensional random walk with correlated dynamical disorder, whose analysis was deemed to be intractable.

In order to calculate $G(t)$, Chatterjee and Loring developed a dynamically disordered Rouse (DDR) model, in which the constraint forces of the FJC model are replaced by harmonic forces.[28] The connection between dynamical freely jointed chain models and harmonic models in the absence of disorder has been well established.[29] In the DDR model, bead mobilities are uncorrelated stochastic variables which fluctuate between zero and a finite value. The model may be viewed as a dynamical generalization of statically disordered Rouse models that have been treated previously.[4,30,31] The DDR model differs from the FJC model in two important and related respects. First, the DDR model does not include a slithering mode, so that a bead in its low mobility state is absolutely immobile. Second, the rate of medium fluctuations is treated as an externally specified parameter, rather than being evaluated self-consistently as a function of chain length. Application of this self-consistent procedure to the DDR model in the absence of a slithering mode yields unphysical results. In Ref. 28, we developed an approximation strategy for determining $G(t)$ within the DDR model that yields a plateau in $G(t)$ for a slowly relaxing medium. Because the medium relaxation rate was not related to the chain length, the crossover from unentangled to entangled behavior as a function of increasing chain length could not be investigated.

In the present work, we generalize the DDR model of Ref. 28 to include a slithering mode and a self-consistent determination of the medium relaxation rate as a function of chain length. We designate this model the DDRS model (dynamically disordered Rouse model with slithering) to facilitate discussion of the comparison to our previous DDR model. A polymer chain in the DDRS model is assumed to move by two dynamical processes. The first is a Rouse motion that is constrained by dynamical obstacles, and the second is a slithering motion that is unaffected by the obstacles. The dynamical obstacles impeding local motions are represented by fluctuations in the bead friction coefficients, as in the DDR model.[28] The slithering rate is taken to be inversely proportional to the chain length, since it mimics a cooperative motion involving the entire chain.[24(b)] Because the relaxation rate of the dynamical obstacles is determined self-consistently from the chain dynamics, its form reflects contributions from both slithering and hindered Rouse motions. For this reason, the slithering motions and Rouse dynamics are *not* treated as independent, uncoupled processes in this model. The Rouse dynamics are influenced by the slithering mode through the relaxation of obstacles, but the slithering mode is unaffected by the local motions.

In the unentangled limit of short chains in which the Rouse motions are not significantly hindered, the slithering motion, while technically present, makes a negligible contribution to dynamical properties. In the strongly entangled limit, the chain moves through a combination of slithering and Rouse motion. In the crossover regime between entangled and unentangled behavior, both slithering and local motions contribute to the dynamics. This model is based on the ansatz that in this crossover regime in which the chain's local motions are not as strongly constrained as in the entangled limit, a slithering motion may still be identified. The validity of this assumption remains to be tested by computer simulations of molecular models of polymer melts. Within the context of the present model, this ansatz may be tested a posteriori through comparison of our calculations to data from laboratory and computer experiments. The FJC model, which contains the same ansatz, has been shown to yield reasonable results for the diffusion coefficient[24(e)] and the dynamic structure factor[24(f)] for systems that are neither unentangled nor strongly entangled. In Sec. II, the DDRS model is defined, and the self-consistent determination of the medium relaxation rate is described. Section III is devoted to the treatment of $G(t)$. Calculations of $G(t)$, the storage and loss moduli, and η are presented and discussed in Sec. IV.

II. THE DDRS MODEL

We represent the polymer by a harmonic chain of N beads whose mobilities fluctuate in time. The mobility of bead j is proportional to a stochastic medium variable σ_j, whose value fluctuates between 0 and 1. The state of the system at time t is specified by the chain configuration $\mathbf{R}=(\mathbf{r}_1,\mathbf{r}_2,...,\mathbf{r}_N)$ and the state of the medium $\boldsymbol{\sigma}=(\sigma_1,\sigma_2,...,\sigma_N)$ at that time. We define $P(\mathbf{R},\boldsymbol{\sigma},t;\mathbf{R}_0)$ to be the probability density that the polymer has configuration $\mathbf{R}$ and the medium has state $\boldsymbol{\sigma}$ at time t, given that the polymer had configuration $\mathbf{R}_0$ at $t=0$, and that the medium was initially at equilibrium. The DDRS model is defined by the following equation of motion for $P(\mathbf{R},\boldsymbol{\sigma},t;\mathbf{R}_0)$:

$$\frac{\partial P(\mathbf{R},\boldsymbol{\sigma},t;\mathbf{R}_0)}{\partial t} = \hat{L}_{\mathrm{DDR}} P(\mathbf{R},\boldsymbol{\sigma},t;\mathbf{R}_0) + \hat{L}_S P(\mathbf{R},\boldsymbol{\sigma},t;\mathbf{R}_0) + \sum_{\boldsymbol{\sigma}'} \Omega_{\boldsymbol{\sigma}\boldsymbol{\sigma}'} P(\mathbf{R},\boldsymbol{\sigma}',t;\mathbf{R}_0) - \kappa(t) \sum_{j=1}^{N} y_j \frac{\partial P(\mathbf{R},\boldsymbol{\sigma},t;\mathbf{R}_0)}{\partial x_j}. \tag{2.1}$$

The final term in Eq. (2.1) represents the time evolution of P due to an externally imposed velocity gradient characterized by strain rate $\kappa(t)$. The operator $\hat{L}_{\mathrm{DDR}}$ in Eq. (2.1) is defined as

$$\hat{L}_{\mathrm{DDR}} P(\mathbf{R},\boldsymbol{\sigma},t;\mathbf{R}_0) = \sum_{j=1}^{N} D_j(\boldsymbol{\sigma}) \nabla_j^2 P(\mathbf{R},\boldsymbol{\sigma},t;\mathbf{R}_0) - \sum_{j,m=1}^{N} \boldsymbol{\nabla}_j \cdot [V_{jm}(\boldsymbol{\sigma}) \mathbf{r}_m P(\mathbf{R},\boldsymbol{\sigma},t;\mathbf{R}_0)]. \tag{2.2}$$

In Eq. (2.2), $V_{jm}(\boldsymbol{\sigma})$ and $D_j(\boldsymbol{\sigma})$ are defined as in Eq. (2.1) of Ref. 28 for the DDR model

$$D_j(\boldsymbol{\sigma}) = \sigma_j [k_B T/\xi], \tag{2.3a}$$

$$V_{jm}(\boldsymbol{\sigma}) = \sigma_j W_{jm}, \tag{2.3b}$$

$$W_{jm} = w[\delta_{j,m-1} + \delta_{j,m+1} - 2\delta_{jm}], \quad 1 < j,m < N, \tag{2.3c}$$

$$W_{1m} = W_{m1} = w[\delta_{m,2} - \delta_{m,1}], \tag{2.3d}$$

$$W_{Nm} = W_{mN} = w[\delta_{m,N-1} - \delta_{m,N}], \tag{2.3e}$$

$$w = 3k_B T/(b^2 \xi). \tag{2.3f}$$

The operator $\hat{L}_{\mathrm{DDR}}$ describes the dynamics of a Rouse chain in which bead j is assigned the mobility σ_j/ξ, with ξ representing the friction coefficient for a mobile bead. The time scale for these dynamics is set by the rate w in Eq. (2.3f), which is proportional to the ratio of the force constant of a harmonic bond to the monomer friction coefficient. The root-mean-squared separation of adjacent beads is denoted b in Eq. (2.3f).

The operator $\hat{L}_S$ in Eq. (2.1) is defined by

$$\hat{L}_S P(\mathbf{R},\boldsymbol{\sigma},t;\mathbf{R}_0) = \frac{w}{4\pi N} \int d\hat{\boldsymbol{\theta}} [P(\mathbf{r}_1 - |\mathbf{b}_N| \hat{\boldsymbol{\theta}}, \mathbf{r}_1, \mathbf{r}_2, \ldots \mathbf{r}_{N-1}, \boldsymbol{\sigma}, t; \mathbf{R}_0) + P(\mathbf{r}_2, \mathbf{r}_3, \ldots, \mathbf{r}_N, \mathbf{r}_N + |\mathbf{b}_2| \hat{\boldsymbol{\theta}}, \boldsymbol{\sigma}, t; \mathbf{R}_0) - 2P(\mathbf{R},\boldsymbol{\sigma},t;\mathbf{R}_0)], \tag{2.4a}$$

$$\mathbf{b}_j = \mathbf{r}_j - \mathbf{r}_{j-1}. \tag{2.4b}$$

In Eq. (2.4), $\hat{\boldsymbol{\theta}}$ represents a unit vector whose orientation is integrated over the surface of the unit sphere, and $\mathbf{b}_j$ denotes the jth bond vector. The operator $\hat{L}_S$ describes the evolution of the distribution function caused by the slithering motion, in which a bead and its associated bond vector are detached from one end of the chain and then reattached at the other end with random orientation of the bond vector. For mathematical convenience, we assume that the length of the bond vector is preserved. This process occurs with a rate w/N that is unaffected by the state of the medium. If the bond vectors were constrained to be of equal length, this mechanism would be identical to the slithering mode introduced in the FJC model.[24(b)] In the absence of $\hat{L}_S$, Eq. (2.1) reduces to the corresponding equation of motion in the DDR model.[28]

The transition matrix $\boldsymbol{\Omega}$ in Eq. (2.1) governs the fluctuations of the medium variables, and is defined as in Ref. 28 for the DDR model

$$\boldsymbol{\Omega}_{\boldsymbol{\sigma}\boldsymbol{\sigma}'} = \sum_j \omega_{\sigma_j \sigma_j'} \prod_{m \neq j} \delta_{\sigma_m \sigma_m'}, \tag{2.5a}$$

$$\omega_{00} = -\omega_{10} = -\gamma c, \tag{2.5b}$$

$$\omega_{11} = -\omega_{01} = -\gamma(1-c). \tag{2.5c}$$

The uncorrelated medium variables fluctuate between the values of 0 and 1 with rate γ. At equilibrium, a medium variable has value 0 with probability 1-c and value 1 with probability c. We refer to 1-c as the obstacle density.

The determination of an ensemble average requires a sequence of three operations. The average of a function of the polymer configuration $F(\mathbf{R})$ over all trajectories of the system consistent with a given final state of the medium $\boldsymbol{\sigma}$ and a given initial chain configuration $\mathbf{R}_0$ is represented by an overbar

$$\bar{F}(\boldsymbol{\sigma},t;\mathbf{R}_0) = \int d\mathbf{R}\, F(\mathbf{R}) P(\mathbf{R},\boldsymbol{\sigma},t;\mathbf{R}_0). \tag{2.6}$$

The average over initial chain configurations is represented by angular brackets

$$\langle \bar{F}(\boldsymbol{\sigma},t) \rangle = \int d\mathbf{R}_0\, \psi_{\mathrm{eq}}(\mathbf{R}_0) \bar{F}(\boldsymbol{\sigma},t;\mathbf{R}_0). \tag{2.7}$$

The equilibrium distribution of initial chain configurations, which is denoted ψ_{eq}, is the Gaussian distribution consistent with a harmonic intrachain potential. The averaging process is completed by summing over all states of the medium at time t

$$\sum_{\boldsymbol{\sigma}} \langle \bar{F}(\boldsymbol{\sigma},t) \rangle. \tag{2.8}$$

The medium variables fluctuate with rate γ, which in our previous study of the DDR model[28] was treated as an externally specified parameter. For the DDRS model, however, we apply the self-consistent strategy used in our treatment of the FJC model[24(e)] to determine γ as a function of chain length and obstacle density. This approach is based on consideration of $C_R(t)$, the autocorrelation function of the chain's end-to-end vector. For the DDRS model, $C_R(t)$ takes the form

$$C_R(t) = \sum_{\boldsymbol{\sigma}} \sum_{j=2}^{N} \sum_{m=2}^{N} \langle \overline{\mathbf{b}_j}(\boldsymbol{\sigma},t;\mathbf{R}_0) \cdot \mathbf{b}_m(0) \rangle. \tag{2.9}$$

An equation of motion for the partially averaged bond vector $\overline{\mathbf{b}_j}(\boldsymbol{\sigma},t;\mathbf{R}_0)$ may be constructed by substituting Eq. (2.1) into the identity

$$\frac{\partial \overline{\mathbf{b}_j}(\boldsymbol{\sigma},t;\mathbf{R}_0)}{\partial t} = \int d\mathbf{R}\ \mathbf{b}_j \frac{\partial P(\mathbf{R},\boldsymbol{\sigma},t;\mathbf{R}_0)}{\partial t}. \tag{2.10}$$

The resulting equations are equivalent to the equations of motion for partially averaged bond vectors in the FJC model, which are presented in Eqs. (2.9a)–(2.9e) of Ref. 24(b). Since the partially averaged bond vectors in the FJC and DDRS models obey the same equations of motion, and since the chains in both models are governed by Gaussian configurational distributions, $C_R(t)$ for the DDRS model is exactly equal to $C_R(t)$ for the FJC model. In the absence of the slithering mode and of disorder ($\hat{L}_S=0$, $c=1$), this connection reduces to the established relationship between $C_R(t)$ in the Rouse model and in the Orwoll–Stockmayer model of a freely-jointed chain.[29]

In Ref. 24(b), $C_R(t)$ was calculated for the FJC model within the dynamical effective medium approximation (EMA),[25–27] and γ was determined by requiring that it equal the smallest configurational relaxation rate that characterizes $C_R(t)$. Applying the EMA to the DDRS model yields the same relation of γ to chain length and obstacle density that was obtained in the FJC model

$$\gamma = w\left(\frac{\pi}{N}\right)^2\left[\frac{1}{N}+\frac{1}{2}-\frac{N}{\alpha\pi N_e}-\frac{1}{\alpha\pi} + \sqrt{\left[\frac{1}{2}-\frac{N}{\alpha\pi N_e}-\frac{1}{\alpha\pi}\right]^2+\frac{2}{\alpha\pi}\left(1-\frac{1}{N_e}\right)}\right], \tag{2.11a}$$

$$\alpha = \sqrt{4+\frac{\pi^2}{N^2}}-\frac{\pi}{N}, \tag{2.11b}$$

$$N_e = 1/(1-c). \tag{2.11c}$$

The entanglement number N_e is defined in Eq. (2.11c) to be the mean number of bonds separating a successive pair of temporarily immobilized beads. The expression for γ in Eq. (2.11) simplifies in the physically relevant case in which N, $N_e \gg 1$. In these circumstances, γ displays the following limiting behavior:

$$\gamma = w\pi^2/N^2, \quad N/N_e \ll 1, \tag{2.12a}$$

$$\gamma = w\pi^2 N_e/N^3, \quad N/N_e \gg 1. \tag{2.12b}$$

For unentangled chains ($N \ll N_e$), the medium relaxation rate equals the slowest conformational relaxation rate of an unhindered Rouse chain. For an entangled fluid ($N \gg N_e$), the medium relaxation rate displays the same N^{-3} dependence that is predicted for the tube disengagement rate in the tube model. The DDRS model is defined by Eqs. (2.1)–(2.5), together with the self-consistently determined value of γ in Eq. (2.11).

III. THE SHEAR MODULUS

We have carried out a linear response calculation that relates the intramolecular contribution to the shear modulus $G(t)$ for the DDR model to equilibrium correlation functions of bead coordinates.[28] The same expression is valid in the DDRS model

$$G(t) = \frac{\rho\xi w}{NK_0}\sum_{j=1}^{N-1}\sum_{\boldsymbol{\sigma}} S_{jj}(\boldsymbol{\sigma},t), \tag{3.1a}$$

$$S_{nm}(\boldsymbol{\sigma},t) = \langle \overline{b^x_{n+1} b^y_{m+1}}(\boldsymbol{\sigma},t)\rangle. \tag{3.1b}$$

In Eqs. (3.1), we have reexpressed Eqs. (2.10) of Ref. 28 in terms of bond vectors. The number density of monomers is denoted ρ. The applied strain rate $\kappa(t)$ in Eq. (2.1) is taken to have the form $K_0\delta(t)$. The x and y components of the bond vector $\mathbf{b}_j$ are denoted b_j^x and b_j^y, respectively. Equations of motion for the quantities $S_{nm}(\boldsymbol{\sigma},t)$ may be derived by differentiating the right side of Eq. (3.1b) with respect to time, and applying the expression for the time derivative of a partially averaged quantity in Eq. (2.10). Introduction of the equation of motion for the distribution function in Eq. (2.1) and the definition of the average over initial polymer configurations in Eq. (2.7) yields

$$\frac{\partial S_{nm}(\boldsymbol{\sigma},t)}{\partial t} = \sum_{j,k=1}^{N-1}[W^R_{nm,jk}(\boldsymbol{\sigma}) + W^S_{nm,jk}]S_{jk}(\boldsymbol{\sigma},t) + \sum_{\boldsymbol{\sigma}'}\Omega_{\boldsymbol{\sigma}\boldsymbol{\sigma}'}S_{nm}(\boldsymbol{\sigma}',t), \tag{3.2a}$$

$$W^R_{nm,jk}(\boldsymbol{\sigma}) = \delta_{nj}K_{mk}(\boldsymbol{\sigma}) + \delta_{mk}K_{nj}(\boldsymbol{\sigma}),$$

$$K_{jk}(\boldsymbol{\sigma}) = w[\sigma_k\delta_{j,k-1} + \sigma_j\delta_{j,k+1} - \delta_{j,k}(\sigma_{j+1}+\sigma_j)], \quad 1<j,k<N-1,$$

$$K_{1k}(\boldsymbol{\sigma}) = K_{k1}(\boldsymbol{\sigma}) = w[\sigma_2\delta_{k2} - \delta_{1k}(\sigma_1+\sigma_2)],$$

$$K_{N-1,k}(\boldsymbol{\sigma}) = K_{k,N-1}(\boldsymbol{\sigma}) = w[\sigma_{N-1}\delta_{k,N-2} - \delta_{N-1,k}(\sigma_{N-1}+\sigma_N)], \tag{3.2b}$$

$$W^S_{nm,jk} = (w/N)[\delta_{n,j+1}\delta_{m,k+1} + \delta_{n,j-1}\delta_{m,k-1} - 2\delta_{nj}\delta_{mk}]. \tag{3.2c}$$

The matrix $\mathbf{W}^R(\boldsymbol{\sigma})$ in Eq. (3.2b) contains the contribution from Rouse dynamics and the matrix $\mathbf{W}^S$ in Eq. (3.2c) reflects the effects of the slithering motion. The solution to Eq. (3.2a) satisfies initial conditions consistent with a harmonic intrachain potential

$$S_{nm}(\boldsymbol{\sigma},0) = \frac{K_0 b^2}{3}\delta_{nm}\Phi(\boldsymbol{\sigma}), \tag{3.3a}$$

$$\Phi(\boldsymbol{\sigma}) = \prod_{j=1}^{N}[c\,\delta_{\sigma_j,1} + (1-c)\,\delta_{\sigma_j,0}]. \tag{3.3b}$$

The equilibrium distribution of medium variables is denoted $\Phi(\boldsymbol{\sigma})$.

The coupled linear differential equations in Eq. (3.2a) may be formally solved by taking Laplace transforms

$$\hat{S}_{nm}(\boldsymbol{\sigma},s) \equiv \int_0^\infty dt\ e^{-st}S_{nm}(\boldsymbol{\sigma},t) = \sum_{j,k=1}^{N-1}\sum_{\boldsymbol{\sigma}'}[\boldsymbol{\Gamma}(s)]_{nm\boldsymbol{\sigma};jk\boldsymbol{\sigma}'}S_{jk}(\boldsymbol{\sigma}',0), \tag{3.4a}$$

$$[\mathbf{\Gamma}^{-1}(s)]_{nm\boldsymbol{\sigma};jk\boldsymbol{\sigma}'} \equiv s\,\delta_{nj}\delta_{mk}\delta_{\boldsymbol{\sigma}\boldsymbol{\sigma}'} - \delta_{\boldsymbol{\sigma}\boldsymbol{\sigma}'}[W^R_{nm,jk}(\boldsymbol{\sigma}) + W^S_{nm,jk}] - \delta_{nj}\delta_{mk}\Omega_{\boldsymbol{\sigma}\boldsymbol{\sigma}'}. \tag{3.4b}$$

The Laplace transform of $S_{nm}(\boldsymbol{\sigma},t)$ is related in Eq. (3.4a) to a propagator $\mathbf{\Gamma}$, which is defined in terms of its inverse in Eq. (3.4b). $\mathbf{\Gamma}$ may be regarded as a square matrix of dimension $2^N(N-1)^2$. Substitution of this formal solution of Eq. (3.2a) into Eq. (3.1a) relates the shear modulus to elements of $\mathbf{\Gamma}$:

$$G(t) = \frac{\rho k_B T}{N} \sum_{n,m=1}^{N-1} \Lambda_{nn,mm}(t), \tag{3.5a}$$

$$\Lambda_{ij,nm}(t) = \sum_{\boldsymbol{\sigma},\boldsymbol{\sigma}'} \mathbf{L}^{-1}[\mathbf{\Gamma}(s)]_{ij\boldsymbol{\sigma};nm\boldsymbol{\sigma}'}\Phi(\boldsymbol{\sigma}'). \tag{3.5b}$$

The operator $\mathbf{L}^{-1}$ denotes inverse Laplace transformation. The $(N-1)^2$-dimensional propagator $\mathbf{\Lambda}$ is the average of $\mathbf{L}^{-1}\mathbf{\Gamma}$ over the 2^N states of the medium.

We next introduce approximations that permit the evaluation of $G(t)$ from Eq. (3.5a). In the case of an ordered medium, $c=1$, the matrices $\mathbf{W}^R(\boldsymbol{\sigma})$ [Eq. (3.2b)] and $\mathbf{W}^S$ [Eq. (3.2c)] commute. In the disordered case, $0<c<1$, these matrices do not commute. If $\mathbf{W}^R(\boldsymbol{\sigma})$ and $\mathbf{W}^S$ commute, the propagator $\mathbf{\Lambda}$ factors into the product of a propagator $\mathbf{\Lambda}^S$ that reflects slithering dynamics and a propagator $\mathbf{\Lambda}^{\mathrm{DDR}}$ that represents the effects of Rouse dynamics. Our first approximation is to impose this factorization for the case with dynamical disorder:

$$\mathbf{\Lambda}(t) = \mathbf{\Lambda}^S(t)\cdot\mathbf{\Lambda}^{\mathrm{DDR}}(t), \tag{3.6a}$$

$$\mathbf{\Lambda}^S(t) = \exp[t\mathbf{W}^S], \tag{3.6b}$$

$$[\mathbf{\Lambda}^{\mathrm{DDR}}(t)]_{ij,nm} = \mathbf{L}^{-1}\sum_{\boldsymbol{\sigma},\boldsymbol{\sigma}'} [\mathbf{\Gamma}^{\mathrm{DDR}}(s)]_{ij\boldsymbol{\sigma};nm\boldsymbol{\sigma}'}\Phi(\boldsymbol{\sigma}'), \tag{3.6c}$$

$$\{[\mathbf{\Gamma}^{\mathrm{DDR}}(s)]^{-1}\}_{ij\boldsymbol{\sigma};nm\boldsymbol{\sigma}'} = s\,\delta_{in}\delta_{jm}\delta_{\boldsymbol{\sigma}\boldsymbol{\sigma}'} - \delta_{\boldsymbol{\sigma}\boldsymbol{\sigma}'}W^R_{ij,nm}(\boldsymbol{\sigma}) - \delta_{in}\delta_{jm}\Omega_{\boldsymbol{\sigma}\boldsymbol{\sigma}'}. \tag{3.6d}$$

Within this approximation, $G(t)$ in Eq. (3.5a) takes the form

$$G(t) = \frac{\rho k_B T}{N}\left\{\sum_{n,m=1}^{N-1}\Lambda^S_{nn,mm}(t)\left[\sum_{j=1}^{N-1}\Lambda^{\mathrm{DDR}}_{mm,jj}(t)\right]\right\}. \tag{3.7}$$

The sum within square brackets in Eq. (3.7) depends on the value of the index m. For an infinitely long polymer, $N\to\infty$, however, the value of this term is independent of m. Our second approximation is to take this term to be independent of m for finite N. In this case, $G(t)$ is proportional to the product of two factors, $g^S(t)$ and $g^{\mathrm{DDR}}(t)$:

$$G(t) = \{N/[(N-1)\rho k_B T]\}g^S(t)g^{\mathrm{DDR}}(t). \tag{3.8}$$

The factor $g^S(t)$ in Eq. (3.8) represents the shear modulus in the absence of Rouse dynamics. This limit may be attained in the present model by setting $c=0$. This contribution to $G(t)$ is given by

$$g^S(t) = \frac{\rho k_B T}{N}\sum_{n,m=1}^{N-1}\Lambda^S_{nn,mm}(t) \tag{3.9a}$$

$$= \frac{2\rho k_B T}{N^2}\sum_{q=1,3,5,\ldots}^{N-1}\mathrm{ctn}^2\left(\frac{q\pi}{2N}\right)\exp[-w\lambda_q t/N], \tag{3.9b}$$

$$\lambda_q = 4\sin^2\left(\frac{q\pi}{2N}\right). \tag{3.9c}$$

The function $g^S(t)$ has the same form as the prediction for $G(t)$ from the tube model.[32] The second factor in Eq. (3.8) has the form of $G(t)$ in the DDR model of Ref. 28:

$$g^{\mathrm{DDR}}(t) = \frac{\rho k_B T}{N}\sum_{n,m=1}^{N-1}\Lambda^{\mathrm{DDR}}_{nn,mm}(t). \tag{3.10}$$

We evaluate this term using the approximate expression presented in Eq. (4.8) of Ref. 28:

$$g^{\mathrm{DDR}}(t) = \frac{\rho k_B T}{N}\,\mathbf{L}^{-1}\sum_{q=1}^{N-1}\frac{1}{s+2w\lambda_q\psi_2^\gamma(s)}, \tag{3.11a}$$

$$\psi_2^\gamma(s) = 1 + \frac{4}{(s+\gamma)\tau_e} - \sqrt{\frac{16}{(s+\gamma)^2\tau_e^2} + \frac{8}{(s+\gamma)\tau_e} + \frac{1}{w\tau_e}}, \tag{3.11b}$$

$$\tau_e = N_e^2/w. \tag{3.11c}$$

The effective medium function ψ_2^γ(s) in Eq. (3.11b) is introduced in Eq. (4.9) of Ref. 28. This quantity may be interpreted as a dimensionless bead mobility whose frequency dependence reflects dynamics of the surrounding molecules. The entanglement time τ_e in Eq. (3.11c) is proportional to the longest relaxation time of a Rouse chain of length equal to the entanglement length N_e, which is defined in Eq. (2.11c).

The calculations of $G(t)$ in Ref. 28 for the DDR model employed the relations in Eqs. (3.11), *with γ treated as an externally controlled parameter*. In the present work, the self-consistently determined value of γ in Eq. (2.11a) is substituted into Eq. (3.11b). This value of γ reflects the effects of both Rouse dynamics in a fluctuating medium and the slithering mode. For this reason, the form of $G(t)$ in Eq. (3.8) does *not* represent a factorization into contributions from two independent processes. The factor $g^S(t)$ in Eq. (3.8) contains the effects of only the slithering motion and is not influenced by Rouse dynamics, while $g^{\mathrm{DDR}}(t)$ represents stress relaxation through both slithering and Rouse dynamics.

Expressions for the storage and loss moduli, denoted $G'(\omega)$ and $G''(\omega)$ respectively, and for the shear viscosity η may be obtained from Eqs. (3.8), (3.9), and (3.11). The storage and loss moduli are defined in terms of $G(t)$ by[3]

$$i\omega\hat{G}(\omega) = G'(\omega) + iG''(\omega), \tag{3.12a}$$

$$\hat{G}(\omega) = \frac{1}{\sqrt{2\pi}}\int_0^\infty dt\; e^{-i\omega t}G(t). \tag{3.12b}$$

The one-sided Fourier transform of $G(t)$ is given by

$$\hat{G}(\omega)=\frac{\sqrt{2}\rho k_B T}{N^3\sqrt{\pi}}\sum_{q_1=1,3,5,\cdots}^{N-1}\mathrm{ctn}^2\left(\frac{q_1\pi}{2N}\right)\times\sum_{q_2=1}^{N-1}\frac{1}{\frac{w\lambda_{q_1}}{N}+i\omega+2w\lambda_{q_2}\psi_2^{\gamma}(i\omega+w\lambda_{q_1}/N)}. \tag{3.13}$$

Equation (3.13) expresses $\hat{G}(\omega)$ in terms of the effective medium function $\psi_2^{\gamma}(z)$ for complex-valued z. This quantity is determined by replacing the real variable s with the complex variable z in Eq. (3.11b), and choosing the branch cut so as to recover the physically relevant solution for real-valued z. The shear viscosity, which equals the time-integral of $G(t)$, may be calculated from Eq. (3.13):

$$\eta=\frac{2\rho k_B T}{N^3}\sum_{q_1=1,3,5,\cdots}^{N-1}\mathrm{ctn}^2\left(\frac{q_1\pi}{2N}\right)\times\sum_{q_2=1}^{N-1}\frac{1}{\frac{w\lambda_{q_1}}{N}+2w\lambda_{q_2}\psi_2^{\gamma}(w\lambda_{q_1}/N)}. \tag{3.14}$$

Numerical calculations of viscoelastic properties from Eqs. (3.8)–(3.14) are presented in Sec. IV.

IV. CALCULATIONS AND DISCUSSION

The shear modulus $G(t)$ is calculated for the DDRS model by numerically performing the summation and inverse Laplace transformation[33] in Eq. (3.11a) to obtain $g^{\mathrm{DDR}}(t)$, by numerically evaluating the summation in Eq. (3.9b) to obtain $g^S(t)$, and by multiplying those quantities as shown in Eq. (3.8). Before discussing numerical results, we consider the limiting behavior displayed by $G(t)$. According to Eq. (3.9), $g^S(t)$ decays with the slithering time τ_S, defined in terms of the Rouse time τ_R by

$$\tau_S=N\tau_R=N^3/(w\pi^2). \tag{4.1}$$

The slithering time has the same scaling with N as the disengagement time in the tube model.[3] The decay of $g^{\mathrm{DDR}}(t)$ in Eq. (3.11) depends on the magnitude of the degree of entanglement, N/N_e. The time dependence of $g^{\mathrm{DDR}}(t)$ is governed by the frequency dependence of the effective medium function ψ_2^{γ} in Eq. (3.11b). This frequency dependence is controlled by the magnitude of $\gamma\tau_e$, with the medium relaxation rate γ defined in Eq. (2.11a) and the entanglement time τ_e defined in Eq. (3.11c).

For the case of an unentangled fluid, $N\ll N_e$, the medium relaxation rate γ is given by the limiting expression in Eq. (2.12a). In this case, $\gamma\tau_e=\pi^2(N_e/N)^2\gg 1$. For $N\ll N_e$ and $N_e\gg 1$, the effective medium function in Eq. (3.11b) has value unity. Substitution of this result into Eq. (3.11a) for $g^{\mathrm{DDR}}(t)$ yields the shear modulus for the Rouse model, which decays as $t^{-1/2}$ for $t\ll\tau_R$, and as e^{-2t/τ_R} for $t\gg\tau_R$.[3] Since $G(t)$ in the Rouse model decays on time scales short compared to τ_S, the slithering process does not contribute significantly to $G(t)$ in the DDRS model for unentangled systems. In the unentangled limit, the DDRS prediction for $G(t)$ reduces to that of the Rouse model.

The shear modulus displays a richer time dependence for an entangled fluid, $N\gg N_e$. In this case, the medium relaxation rate is given by the limiting form in Eq. (2.12b), and the parameter $\gamma\tau_e=\pi^2(N_e/N)^3\ll 1$. For $\gamma\tau_e\ll 1$, the frequency dependence of the effective medium function becomes significant, and $g^{\mathrm{DDR}}(t)$ shows a more complex time dependence than does the shear modulus of the Rouse model. We briefly review the predictions of the DDR model in this limit, which are discussed in Ref. 28. For $t\ll\tau_e$, $g^{\mathrm{DDR}}(t)$ follows the prediction of the Rouse model. At $t\sim\tau_e$, a plateau begins at the plateau modulus

$$G^{(0)}=\rho k_B T/N_e. \tag{4.2}$$

The entanglement number of a laboratory polymer, defined as the ratio of entanglement molecular weight to monomer mass, is conventionally equated to $\rho k_B T/G^{(0)}$.[3] Comparing this relation to Eq. (4.2) establishes the equivalence between the entanglement number in our model, defined in Eq. (2.11c), and the entanglement number for a laboratory polymer. The plateau extends to a time scale γ^{-1}, and is followed by a $t^{-1/2}$ decay up to a renormalized Rouse time, τ_{RR}:

$$\tau_{\mathrm{RR}}=8\tau_R/(\gamma\tau_e)=8N^5/(w\pi^4N_e^3). \tag{4.3}$$

The renormalized Rouse time may be interpreted as the longest relaxation time of a Rouse chain of length N/N_e for which the rate of local motions is γ. In the language of the tube model, this time corresponds to the longest Rouse relaxation time of the tube. For $t\gg\tau_{\mathrm{RR}}$, $g^{\mathrm{DDR}}(t)$ decays exponentially with time constant $\tau_{\mathrm{RR}}/2$. The shear modulus $G(t)$ is proportional to the product of $g^{\mathrm{DDR}}(t)$ and $g^S(t)$. Since $\tau_S\gg\gamma^{-1}$ for an entangled fluid, $g^S(t)$ does not contribute significantly to $G(t)$ until after the times over which the plateau is established. The nature of the decay following the plateau is controlled by the magnitude of $\tau_{\mathrm{RR}}/\tau_S$:

$$\tau_{\mathrm{RR}}/\tau_S=8N^2/(\pi^2N_e^3). \tag{4.4}$$

The value of this ratio depends on the relative magnitudes of N and $N_e^{3/2}$. If $N\ll N_e^{3/2}$, $\tau_{\mathrm{RR}}/\tau_S\ll 1$, and $g^S(t)$ does not contribute significantly to $G(t)$. In this case, $G(t)$ displays the post-plateau time-dependence just described for $g^{\mathrm{DDR}}(t)$. If $N\gg N_e^{3/2}$, $\tau_{\mathrm{RR}}/\tau_S\gg 1$, and $g^S(t)$ contributes significantly to $G(t)$. Under these circumstances, the post-plateau $t^{-1/2}$ decay persists to $t\sim\tau_S$, and is followed by exponential decay with time constant τ_S.

Calculations of $G(t)$ for three different melts are shown by the solid curves in Fig. 1. For the leftmost curve, $N=100$ and $N_e=10^3$. For this unentangled case, $G(t)$ decays in accordance with the prediction of the Rouse model, and does not exhibit a plateau. The middle curve was calculated for $N=500$ and $N_e=100$. For this fluid of intermediate degree of entanglement, $G(t)$ shows Rouse behavior for $t\ll\tau_e$. At later times, $G(t)$ displays an inflection point and the beginnings of a plateau, which is followed by a more rapid decay for $t>\gamma^{-1}$. The leftmost vertical dot–dashed line indicates the value of γ^{-1} for this calculation. For this system, $\tau_{\mathrm{RR}}/\tau_S<1$,

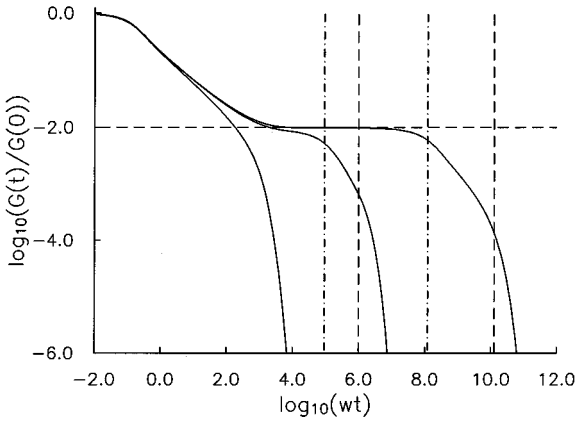

FIG. 1. The time dependence of the viscoelastic shear modulus is calculated from Eq. (3.8) for $N=100$ and $N_e=1000$ (leftmost curve), for $N=500$ and $N_e=100$ (middle curve), and for $N=5000$ and $N_e=100$ (rightmost curve). The time axis is scaled by w in Eq. (2.3f). The leftmost vertical dot–dashed line shows the medium relaxation time γ^{-1} for the parameters of the middle curve, and the rightmost vertical dot–dashed line shows this quantity for the parameters of the rightmost curve. The leftmost vertical dashed line shows the renormalized Rouse time τ_{RR} of Eq. (4.3) for the parameters of the middle curve, and the rightmost vertical dashed line shows the slithering time τ_S of Eq. (4.1) for the parameters of the rightmost curve. The horizontal dashed line shows the plateau modulus $G^{(0)}$ of Eq. (4.2). These calculations illustrate the crossover from relaxation in an unentangled fluid to relaxation in an entangled system.

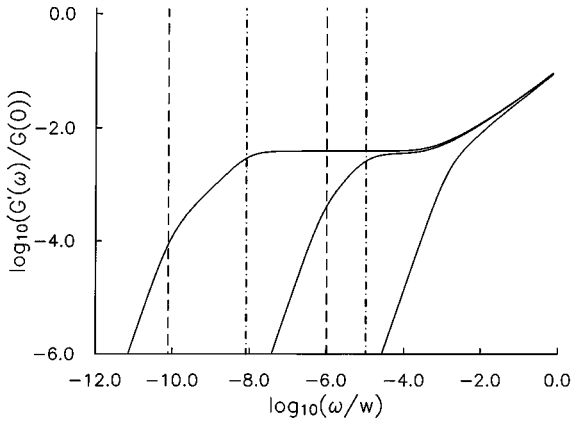

FIG. 2. The frequency dependence of the storage modulus is shown for the same systems considered in Fig. 1. For the leftmost curve, $N=5000$ and $N_e=100$, for the middle curve, $N=500$ and $N_e=100$, and for the rightmost curve, $N=100$ and $N_e=1000$. The leftmost and rightmost vertical dot–dashed lines show the medium relaxation rate γ for the parameters of the leftmost and middle curves. The leftmost vertical dashed line shows τ_S^{-1} for the leftmost curve and the rightmost vertical dashed line shows $\tau_{\mathrm{RR}}{}^{-1}$ for the middle curve.

so that τ_{RR} is the relevant time scale for the post-plateau decay. The leftmost vertical dashed line indicates the value of τ_{RR} for this calculation. For $t \gg \tau_{\mathrm{RR}}$, $G(t)$ decays exponentially. The rightmost solid curve shows $G(t)$ for a strongly entangled fluid with $N=5000$ and $N_e=100$. This curve shows a pronounced plateau at the value $G^{(0)}$ in Eq. (4.2), which is indicated by the horizontal dashed line. This plateau begins to decay at $t \sim \gamma^{-1}$, which is represented by the rightmost vertical dot–dashed line. For this fluid, $\tau_{\mathrm{RR}}/\tau_S > 1$, so that the terminal decay of $G(t)$ has time constant τ_S. The rightmost vertical dashed line shows τ_S for $N=5000$, $N_e=100$.

The storage and loss moduli, defined in Eq. (3.12a), contain the same information as $G(t)$ but in a form more readily compared to results of modern rheological experiments. The storage modulus $G'(\omega)$ is plotted in Fig. 2 for the same three systems investigated in Fig. 1. The leftmost solid curve was calculated for an entangled fluid with $N=5000$ and $N_e=100$. In this case, $G'(\omega)$ displays a plateau for $\gamma < \omega < \tau_e^{-1}$. For these parameters, τ_S^{-1} is indicated by the leftmost vertical dashed line and γ is shown by the leftmost vertical dot–dashed line. The middle solid curve shows $G'(\omega)$ for a system of intermediate degree of entanglement with $N=500$ and $N_e=100$. The rightmost vertical dashed line shows τ_{RR}^{-1} and the rightmost vertical dot–dashed line shows γ for these parameters. The vestigial plateau shown by this curve corresponds to that shown by the $G(t)$ calculation in Fig. 1. The rightmost curve shows $G'(\omega)$ for an unentangled fluid with $N=100$ and $N_e=10^3$. This curve reproduces the predictions of the Rouse model, and shows no plateau.

The loss moduli of the three fluids investigated in Figs. 1 and 2 are shown in Fig. 3. The leftmost and middle solid curves were calculated for $N=5000$ and for $N=500$, respectively. In both of these curves, $N_e=100$. The leftmost dashed vertical line shows τ_S^{-1}, and the leftmost dot–dashed vertical line shows γ for the parameters of the leftmost solid curve. The rightmost dashed vertical line shows τ_{RR}^{-1}, and the rightmost dot–dashed vertical line shows γ for the parameters of the middle solid curve. The rightmost solid curve shows $G''(\omega)$ for an unentangled fluid with $N=100$ and $N_e=10^3$. The middle and leftmost curves show Rouse behavior at high frequencies, but also display a low-frequency feature that is peaked at approximately $\omega \sim \gamma$. The ''valley'' separating the low-frequency peak from the Rouse feature becomes deeper and wider as N is increased at fixed N_e.

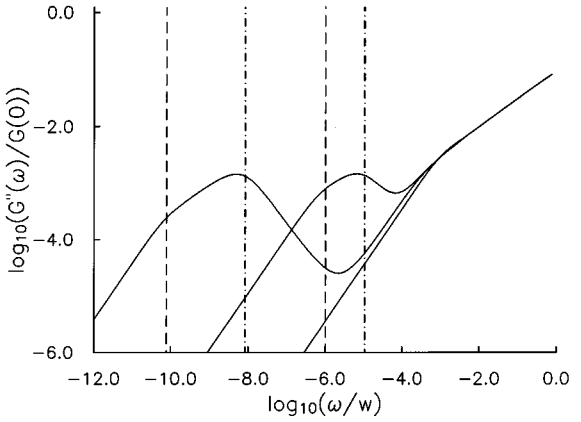

FIG. 3. The frequency dependence of the loss modulus is shown for the same systems considered in Figs. 1 and 2. For the leftmost curve, $N=5000$ and $N_e=100$, for the middle curve, $N=500$ and $N_e=100$, and for the rightmost curve, $N=100$ and $N_e=1000$. The vertical lines have the same significance as in Fig. 2.

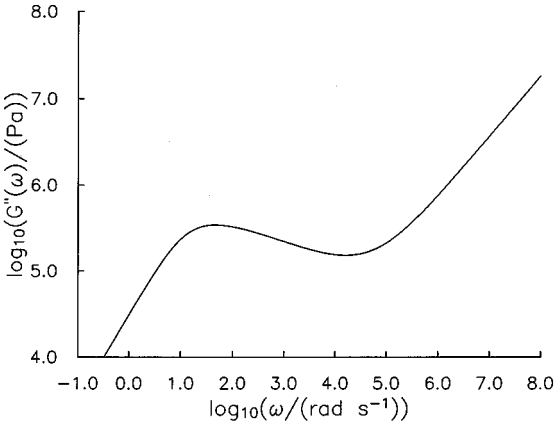

FIG. 4. The loss modulus for polybutadiene with $N/N_e=50$ at 28 °C is calculated from the empirical fitting function of Winter *et al.* in Eq. (3) of Ref. 5.

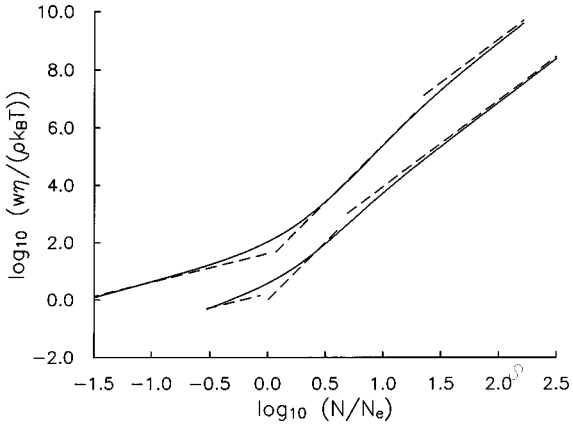

FIG. 5. The chain-length dependence of the coefficient of shear viscosity is calculated from Eq. (3.14) for $N_e=20$ (lower curve) and $N_e=500$ (upper curve). η is scaled by $w/(\rho k_B T)$, with w defined in Eq. (2.3f) and ρ the monomer density. The three dashed line segments adjacent to each curve show the Rouse limit for unentangled chains, the N^4 dependence predicted in Eq. (4.5), and the N^3 dependence predicted in Eq. (4.6).

Winter *et al.* have developed an empirical fitting function for the spectrum of relaxation times in a melt of flexible linear polymers, and have demonstrated that the viscoelastic moduli predicted from this expression agree well with rheological measurements on entangled melts of polystyrene and polybutadiene.[5] We have used Eq. (3) of Ref. 5 together with parameters in Table 4 of Ref. 5 to calculate the loss modulus for polybutadiene with $N/N_e=50$ at 28 °C. The result is shown in Fig. 4. Comparison of the DDRS calculation for $N/N_e=50$ in Fig. 3 to the result in Fig. 4 shows that the DDRS result reproduces qualitatively the low-frequency feature of the spectrum in Fig. 4. The agreement is not quantitative, as the DDRS calculation overestimates the depth and incorrectly predicts the shape of the valley between the low-frequency peak and the Rouse feature. The origin of this discrepancy may be understood by considering our prediction for $G(t)$. As shown in Fig. 1, $G(t)$ displays a rigorous plateau for sufficiently large N/N_e. Over the range of times for which this plateau persists, no stress relaxation is predicted to occur. In the language of the DDRS model, chain dynamics are frozen until the obstacles have relaxed. Since a laboratory liquid is not rigorously immobile on this range of time scales, the true $G''(\omega)$ shows greater intensity for intermediate frequencies than does our calculated result.

The coefficient of shear viscosity may be calculated for the DDRS model from Eq. (3.14). Before discussing numerical calculations, we analyze the limiting behavior predicted by this expression. For an unentangled fluid with $N \ll N_e$, the effective medium function ψ_2^γ in Eq. (3.14) may be replaced by unity. In this limit, Eq. (3.14) reduces to the prediction of the Rouse model, in which $\eta \sim N$. We may estimate η for an entangled fluid by truncating the summation over q_1 in Eq. (3.14) at $q_1=1$. In discussing Eq. (4.4), we noted that the terminal decay of $G(t)$ is controlled by the relative magnitudes of N and $N_e^{3/2}$. The relative magnitudes of these quantities also determine the dependence of η on N. If $N_e \ll N \ll N_e^{3/2}$, the summation over q_2 in Eq. (3.14) may be performed after linearizing the sine function entering in λ_{q_2} to yield

$$\eta=[\rho k_B T/(2w\pi^2)]N^4 N_e^{-3}. \tag{4.5}$$

If N_e is sufficiently large that a significant range of N lies between N_e and $N_e^{3/2}$, η is predicted to scale as N^4. For $N \gg N_e^{3/2}$, the sum over q_2 in Eq. (3.14) may be transformed to an integral to give

$$\eta=[\rho k_B T/(w\pi^2)]N^3 N_e^{-3/2}. \tag{4.6}$$

In the limit of arbitrarily large N/N_e, η is predicted to scale as N^3, as predicted by the tube model. For intermediate N, η may be expected to display a dependence on N that is stronger than N^3 but weaker than N^4.

Calculations of the dependence of η on chain length are shown in Fig. 5 for $N_e=20$ (lower curve) and $N_e=500$ (upper curve). These calculations were performed by evaluating the right side of Eq. (3.14) numerically. Three dashed line segments adjacent to each curve show the limiting behavior just described. The lowest dashed line indicates the Rouse limit, the middle dashed line shows the prediction of Eq. (4.5), and the upper dashed line represents the asymptotic limit shown in Eq. (4.6). For $N_e=20$ and for small N, η displays an N-dependence stronger than that predicted by the Rouse model. The Rouse limit is never quite attained in this curve, since the condition $N \ll 20$ cannot be satisfied. Over an intermediate regime of chain length, η varies with N more weakly than N^4, but more strongly than N^3. For $N \gg N_e^{3/2}$, η shows the asymptotic N^3 dependence indicated by Eq. (4.6). A value of $N_e=500$ is sufficiently large that the Rouse limit is attained for $N \ll N_e$. This value is also sufficiently large that for $N \sim N_e$, η crosses over to the N^4 behavior of Eq. (4.5), which is followed for $N \gg N_e^{3/2}$ by the asymptotic N^3 dependence.

Our prediction for the N dependence of η for an entangled fluid is consistent with the conjecture of Graessley[22]

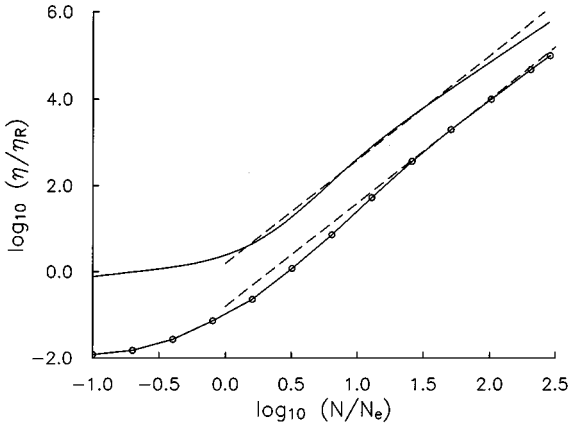

FIG. 6. The calculation of η from Eq. (3.14) is compared to results from the simulation of the tube model by Ball and O'Connor in Ref. 12. The viscosity is scaled by the prediction of the Rouse model, η_R. The upper solid curve shows the DDRS result for $N_e=50$. The adjacent dashed line shows $\eta/\eta_R \sim N^{2.4}$. The circles show data from Table II of Ref. 12, and the solid curve passing through these points is a guide to the eye. The adjacent dashed line shows $\eta/\eta_R \sim N^{2.4}$.

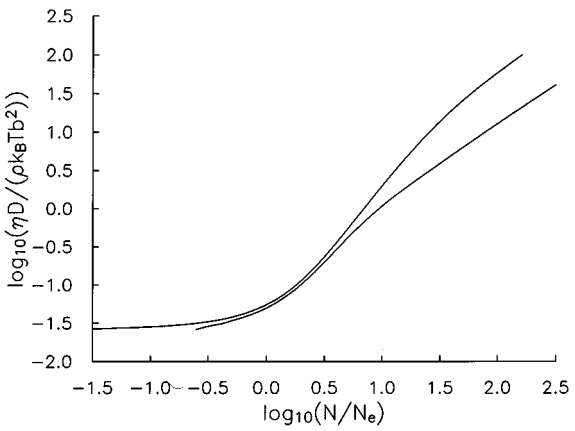

FIG. 7. The product of the coefficients of shear viscosity and self-diffusion for the DDRS model is plotted versus chain length for $N_e=20$ (lower curve) and $N_e=500$ (upper curve). ηD is scaled by $(\rho k_B T b^2)^{-1}$, with ρ the monomer density and b the equilibrium root-mean-squared interbead separation.

and with simulations of the Doi–Edwards tube model.[11,12] O'Connor and Ball[12] have simulated $G(t)$ for a Rouse chain confined to a tube and have found that η scales approximately as $N^{3.4}$ for intermediate chain lengths and as N^3 in the asymptotic limit of long chains. Their results, taken from Table II of Ref. 12, are shown by the circles in Fig. 6. The curve connecting these points is a guide to the eye. The viscosity in this figure is scaled by the viscosity for the Rouse model, η_R. These data do not recover the Rouse limit for $N \ll N_e$, since the tube model does not include that limit. A result that interpolates between Rouse and tube-model limits may be obtained by adding the Rouse viscosity to these data.[12] It has been established that the prediction of $G(t)$ within the tube model decays too slowly, producing a viscosity that is too large relative to experimental results.[12] O'Connor and Ball have adopted the proposal of des Cloizeaux to equate $G(t)$ to the square of the shear modulus predicted by the tube model.[10] This procedure reduces the viscosity to produce good agreement with laboratory data. The data shown in Fig. 6 have been treated by this method. The dashed line adjacent to the O'Connor–Ball calculation shows $\eta/\eta_R \sim N^{2.4}$. Pearson *et al.*[7] have shown that the O'Connor–Ball calculations agree well with measurements of η for entangled fluids of hydrogenated polybutadiene. Our comparison of the DDRS results to those of O'Connor and Ball is thus equivalent to a comparison with the data of Pearson *et al.* The upper solid curve shows the DDRS calculation for $N_e=50$. The adjacent dashed line shows $\eta/\eta_R \sim N^{2.4}$. The DDRS calculation overestimates η, but predicts an N-dependence similar to that shown by the simulation data and the laboratory measurements. A significant discrepancy between the DDRS results and experimental data concerns the chain length at which the crossover from Rouse to entangled dynamics occurs, N_c. For most experimental systems, $N_c \approx 2N_e$, while for the DDRS calculation $N_c \approx N_e$.

Pearson *et al.* have illustrated the onset of entanglement effects in melts of hydrogenated polybutadiene by plotting the product of η and the self-diffusion coefficient D vs N/N_e.[7] The diffusion coefficient, D, for the DDRS model, may be calculated by generalizing the procedure discussed in Sec. II for the calculation of $C_R(t)$ to obtain the time-dependent mean-squared displacement of a bead. This calculation reveals that D for the DDRS model is identically equal to D for the FJC model. We may therefore compute D in the DDRS model from Eq. (2.15) of Ref. 24(e), which represents an approximate calculation based on the FJC model. This result predicts that $D \sim N^{-1}$ for $N \ll N_e$ in agreement with the Rouse model, and that $D \sim N_e N^{-2}$ for $N \gg N_e$, in agreement with the tube model. This expression for D has been shown to agree well with results of computer simulations and laboratory measurements.[24(e)] Figure 7 shows plots of ηD for $N_e=20$ (lower curve) and for $N_e=500$ (upper curve). For $N \ll N_e$, this product is independent of N, and for $N \gg N_e^{3/2}$, $\eta D \sim N$. For $N \sim N_e$, it displays a dependence intermediate between N and N^2. Within the DDRS model, ND is a universal function of N/N_e for N, $N_e \gg 1$, but η/N is not, as shown in Fig. 6. For this reason, ηD is not a universal function of N/N_e in the DDRS model. Both experiment and simulation[34] suggest that ND is a universal function of N/N_e. Rheological measurements[6] on melts of very long polybutadiene chains suggest that this may not be the case for η/N.

We have established that the DDRS model, within the approximate treatment described here, provides a qualitatively correct description of the crossover from unentangled to entangled behavior in the viscoelastic properties of polymer melts. However, the prediction of a rigorous plateau in the shear modulus for sufficiently entangled systems disagrees with the behavior of laboratory polymers, which are not immobile on these time scales. In our treatment of the DDRS model, each Rouse mode relaxes according to a frequency-dependent friction, the inverse of $\psi_2^{\gamma}(s)$ in Eq.

(3.11b), that is independent of the wave vector of the mode. On time scales over which long-wavelength motions are hindered, dynamics on shorter wavelengths are affected by the same effective friction. We believe that the refinement of our treatment of the DDRS model to include a friction coefficient that depends on wave vector as well as frequency[17] will provide a more quantitative description of melt dynamics. This procedure has the potential to allow modes of short wavelength to feel a lower effective friction than modes of longer wavelength. The challenge of introducing a wave vector-dependent friction coefficient in our solution of the DDRS model remains for future work.

ACKNOWLEDGMENTS

Acknowledgment is made to the donors of the Petroleum Research Fund, administered by the American Chemical Society, for partial support of this research. We acknowledge the Cornell University Materials Science Center for project support and for support of P.L.G. through the NSF-REU program.

[1] T. P. Lodge, N. A. Rotstein, and S. Prager, Adv. Chem. Phys. **79**, 1 (1990).
[2] W. W. Graessley, Adv. Polym. Sci. **47**, 67 (1982).
[3] M. Doi and S. F. Edwards, *The Theory of Polymer Dynamics* (Oxford University, Oxford, 1986).
[4] M. Rubinstein and R. H. Colby, J. Chem. Phys. **89**, 5291 (1988).
[5] J. K. Jackson, M. E. De Rosa, and H. H. Winter, Macromolecules **27**, 2426 (1994).
[6] R. H. Colby, L. J. Fetters, and W. W. Graessley, Macromolecules **20**, 2226 (1987); D. S. Pearson, G. VerStrate, E. von Meerwall, and F. Schilling, Macromolecules **20**, 1133 (1987).
[7] D. S. Pearson, L. J. Fetters, W. W. Graessley, G. VerStrate, and E. von Meerwall, Macromolecules **27**, 711 (1994).
[8] P. G. de Gennes, J. Chem. Phys. **55**, 572 (1971).
[9] M. Doi, J. Polym. Sci. Polym. Phys. Ed. **21**, 667 (1983).
[10] J. des Cloizeaux, Macromolecules **23**, 4678 (1990); **25**, 835 (1992).
[11] R. Ketzmerick and H. C. Ottinger, Continuum Mech. Thermodyn. **1**, 113 (1989).
[12] N. P. T. O'Connor and R. C. Ball, Macromolecules **25**, 5677 (1992).
[13] H. Watanabe and M. Tirrell, Macromolecules **22**, 927 (1989).
[14] T. A. Kavassalis and J. Noolandi, Macromolecules **21**, 2869 (1988).
[15] J. F. Douglas and J. B. Hubbard, Macromolecules **24**, 3163 (1991).
[16] P. Tong and M. F. Herman, Macromolecules **26**, 3727, 3733 (1993); M. F. Herman, J. Chem. Phys. **103**, 4324 (1995).
[17] K. S. Schweizer, Phys. Scr. T **49**, 99 (1993); K. S. Schweizer and G. Szamel, Philos. Mag. B **71**, 783 (1995); J. Chem. Phys. **103**, 1934 (1995).
[18] R. B. Bird and H. C. Ottinger, Annu. Rev. Phys. Chem. **43**, 371 (1992).
[19] U. Genz and T. Vilgis, J. Chem. Phys. **101**, 7111 (1994).
[20] M. Rubinstein, Phys. Rev. Lett. **59**, 1946 (1987).
[21] G. T. Barkema, J. F. Marko, and B. Widom, Phys. Rev. E **49**, 5303 (1994).
[22] W. W. Graessley, J. Polym. Sci. **18**, 27 (1980).
[23] G. H. Weiss, J. T. Bendler, and M. F. Schlesinger, Macromolecules **21**, 521 (1988).
[24] (a) R. F. Loring, J. Chem. Phys. **94**, 1505 (1991); (b) I. Szleifer and R. F. Loring, *ibid*. **95**, 2080 (1991); (c) I. Szleifer, J. D. Wilson, and R. F. Loring, *ibid*. **95**, 8474 (1991); (d) J. D. Wilson and R. F. Loring, *ibid*. **97**, 3710 (1992); (e) **99**, 7150 (1993); (f) A. P. Chatterjee and R. F. Loring, *ibid*. **101**, 1595 (1994); (g) J. D. Wilson and R. F. Loring, *ibid*. **103**, 1641 (1995).
[25] A. K. Harrison and R. Zwanzig, Phys. Rev. A **32**, 1072 (1985).
[26] M. Sahimi, J. Phys. C **19**, 1311 (1986).
[27] A. Nitzan and M. A. Ratner, J. Phys. Chem. **98**, 1765 (1994).
[28] A. P. Chatterjee and R. F. Loring, J. Chem. Phys. **103**, 4711 (1995).
[29] See Ref. 3, p. 129.
[30] J. Skolnick and R. Yaris, J. Chem. Phys. **88**, 1418 (1988).
[31] J. des Cloizeaux, J. Phys. I (Paris) **3**, 1523 (1993).
[32] See Ref. 3, p. 226.
[33] H. Stehfest, Commun. ACM **13**, 47, 624 (1970).
[34] K. Kremer and G. S. Grest, J. Chem. Phys. **92**, 5057 (1990).